1521-0103/12/3412-350–359$25.00
THE JOURNAL OF PHARMACOLOGY AND EXPERIMENTAL THERAPEUTICS Vol. 341, No. 2
190769/3762459
JPET 341:350–359, 2012

VUF10166, a Novel Compound with Differing Activities at 5-HT_3A and 5-HT_3AB Receptors

A. J. Thompson, M. H. P. Verheij, I. J. P. de Esch, and S. C. R. Lummis

Department of Biochemistry, University of Cambridge, Cambridge, United Kingdom (A.J.T., S.C.R.L.); and Medicinal Chemistry, VU University of Amsterdam, Amsterdam, The Netherlands (M.H.P.V., I.J.P.d.E.)

Received December 4, 2011; accepted January 9, 2012

ABSTRACT

The actions of a novel, potent 5-HT_3 receptor ligand, [2-chloro-(4-methylpiperazine-1-yl)quinoxaline (VUF10166)], were examined at heterologously expressed human 5-HT_3A and 5-HT_3AB receptors. VUF10166 displaced [^{3}H]granisetron binding to 5-HT_3A receptors expressed in human embryonic kidney cells with high affinity (K_i = 0.04 nM) but was less potent at 5-HT_3AB receptors (K_i = 22 nM). Dissociation of [^{3}H]granisetron in the presence of VUF10166 was best fit with a single time constant ($t_{1/2}$ = 53 min) at 5-HT_3A receptors, but with two time constants ($t_{1/2}$ = 55 and 2.4 min) at 5-HT_3AB receptors. Electrophysiological studies in oocytes revealed that VUF10166 inhibited 5-HT-induced responses at 5-HT_3A receptors at nanomolar concentrations, but inhibition and recovery were too slow to determine an IC_{50}. At 5-HT_3AB receptors, inhibition and recovery were faster, yielding an IC_{50} of 40 nM. Cysteine substitutions in the complementary (−), but not the principal (+), face of the 5-HT_3B subunit produced heteromeric receptors in which the actions of VUF10166 resembled those at homomeric receptors. At 5-HT_3A receptors, VUF10166 at higher concentrations also behaved as a partial agonist (EC_{50} = 5.2 μM; R_{max} = 0.24) but did not elicit significant responses at 5-HT_3AB receptors at ≤100 μM. Thus, we propose that VUF10166 binds to the common A+A− site of both receptor types and to a second A+B− modulatory site in the heteromeric receptor. The ability of VUF10166 to distinguish between 5-HT_3A and 5-HT_3AB receptors could help evaluate differences between these receptor types and has potential therapeutic value.

Introduction

5-HT_3 receptors belong to a family of membrane-bound proteins responsible for inhibitory and excitatory fast synaptic neurotransmission in the central and peripheral nervous systems. The family also includes nicotinic acetylcholine (nACh), GABA, and glycine receptors. All of these receptors are composed of five subunits that assemble around a central ion-conducting pore. To date, genes for five different 5-HT_3 receptor subunits (A–E) have been identified. Only the A subunit can form homomeric receptors, and it can also combine with subunits B to E to produce functional heteromeric receptors, although only receptors containing A and AB subunits have been extensively characterized (Davies et al., 1999; Niesler et al., 2007; Holbrook et al., 2009). Each subunit contains an extracellular domain that is responsible for ligand binding, a transmembrane domain that allows ions to pass through the cell membrane, and an intracellular domain that is involved in intracellular modulation and channel conductance. The agonist binding site is located in the extracellular domain at the interface of two adjacent subunits. It is formed by the convergence of three amino acid loops (loops A–C) from one subunit (+ or principal face) and three β-strands (loops D–F) from the adjacent subunit (− or complementary face) (Barnes et al., 2009; Thompson et al., 2010a).

Competitive antagonists of 5-HT_3 receptors, such as tropisetron and ondansetron, are used to treat emesis and irritable bowel syndrome, and a range of other therapeutic uses have been proposed (Thompson and Lummis, 2007; Walstab et al., 2010). The pharmacology of these competitive ligands is almost identical at 5-HT_3A and 5-HT_3AB receptors, and to date none can be used to distinguish homomeric from heteromeric receptors (Brady et al., 2001). In contrast, the potencies of noncompetitive antagonists that bind to the channels of 5-HT_3A and 5-HT_3AB receptors are different (Das and Dillon, 2005; Thompson and Lummis, 2008; Thompson et al., 2011a). In other Cys-loop receptors, the identification of li-

This work was supported by the Wellcome Trust [Grant 81925] (to S.C.R.L.); and the European Union [FP7 Grant NeuroCypres] (to S.C.R.L. and I.J.P.d.E.). S.C.R.L. is a Wellcome Trust Senior Research Fellow in Basic Biomedical Science.

Article, publication date, and citation information can be found at http://jpet.aspetjournals.org.

http://dx.doi.org/10.1124/jpet.111.190769.

ABBREVIATIONS: 5-HT, 5-hydroxytryptamine; nACh, nicotinic acetylcholine; VUF10166, 2-chloro-(4-methylpiperazine-1-yl)quinoxaline; MTSEA, (2-aminoethyl)-methanethiosulfonate; HEK, human embryonic kidney; RG3487, *N*-[(3*S*)-1-azabicyclo[2.2.2]oct-3-yl]-1*H*-indazole-3-carboxamide hydrochloride.

gands with subtype specificity has been pharmacologically and therapeutically important (e.g., benzodiazepines and pentobarbital), and the identification of comparable 5-HT$_3$ receptor ligands has the potential to be similarly useful (for review, see Jensen et al., 2008; Walstab et al., 2010). Here, we use radioligand binding and two-electrode voltage-clamp electrophysiology to examine the effects of such a ligand, 2-chloro-(4-methylpiperazine-1-yl)quinoxaline (VUF10166) (Fig. 1), previously identified from a compound fragment screen (Thompson et al., 2010b) at 5-HT$_3$A and 5-HT$_3$AB receptors.

Materials and Methods

Materials. All cell culture reagents were obtained from Invitrogen Ltd. (Paisley, UK), except fetal calf serum, which was from Labtech International (Ringmer, UK). Human 5-HT$_3$A (accession number: P46098) and 5-HT$_3$B (O95264) receptor subunit cDNA were the gift of J. A. Peters (University of Dundee, Dundee, UK). The α7 nACh-5-HT$_3$ chimera is described in Eiselé et al. (1993). The cysteine-reactive compound (2-aminoethyl)-methanethiosulfonate (MTSEA) was purchased from Biotium (Hayward, CA). [^{3}H]Granisetron (63.5 Ci/mmol) and [^{3}H]epibatidine (55.8 Ci/mmol) were from PerkinElmer Life and Analytical Sciences (Cambridge, UK).

Cell Culture and Oocyte Maintenance. *Xenopus laevis* oocyte-positive females were purchased from Nasco (Fort Atkinson, WI) and maintained according to standard methods (Goldin, 1992). Harvested stage V to VI *X. laevis* oocytes were washed in four changes of ND96 (96 mM NaCl, 2 mM KCl, 1 mM $MgCl_2$, and 5 mM HEPES, pH 7.4, with NaOH), defolliculated in 1.5 mg/ml collagenase type 1A for 2 h, washed again in four changes of ND96, and stored in ND96 containing 2.5 mM sodium pyruvate, 50 mM gentamicin, and 0.7 mM theophylline.

Human embryonic kidney (HEK) 293 cells were maintained on 90-mm tissue culture plates at 37°C and 7% CO_2 in a humidified atmosphere. They were cultured in Dulbecco's modified Eagle's medium/nutrient mix F12 with GlutaMAX I media (1:1; Invitrogen) containing 10% fetal calf serum. For radioligand binding studies, cells in 90-mm dishes were transfected using polyethyleneimine and were incubated for 2 to 3 days before harvesting as described previously (Thompson et al., 2011b).

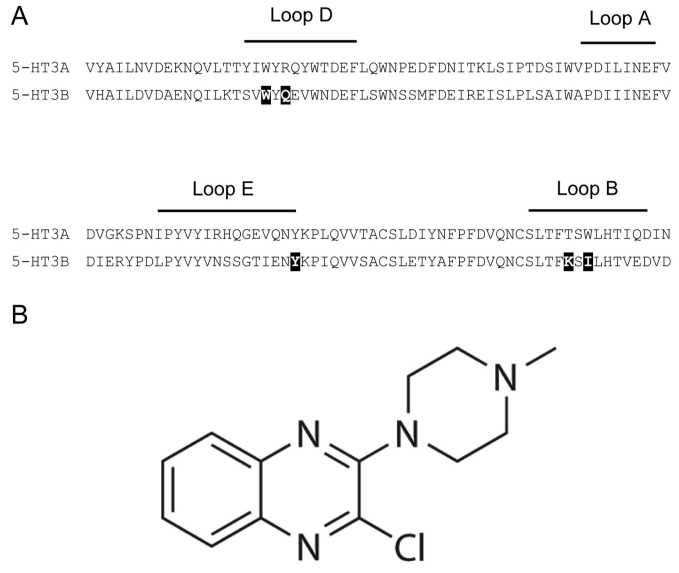

Fig. 1. A, an alignment of 5-HT$_3$A and 5-HT$_3$B subunit residues. B subunit residues that were Cys-substituted in this study are shown as white text on a black background. The effects of these residues on 5-HT activation and [^{3}H]granisetron binding have already been studied elsewhere (Thompson et al., 2011b), and each aligns with an A subunit residue that has been shown to be an important binding site residue (for review, see Thompson et al., 2010a). B, structure of VUF10166.

Receptor Expression. Human 5-HT$_3$A and 5-HT$_3$B subunit cDNA was cloned into pGEMHE for oocyte expression (Liman et al., 1992) and pcDNA3.1 (Invitrogen, Paisley, UK) for expression in HEK 293 cells. Mutagenesis (Fig. 1A) was performed using QuikChange (Agilent Technologies, Santa Clara, CA). To facilitate comparisons with previous work, we use the numbering of the equivalent residues in the mouse 5-HT$_3$A subunit; for human 5-HT$_3$B, 7 should be subtracted from the residue number. cRNA was in vitro-transcribed from cDNA using the mMESSAGE mMACHINE T7 Transcription Kit (Ambion, Austin, TX). Stage V and VI oocytes were injected with 50 nl of ~400 ng/μl cRNA, and currents were recorded 1 to 4 days after injection. A ratio of 1:3 (A/B) was used for the expression of heteromeric receptors.

Electrophysiology. With use of two-electrode voltage-clamp electrophysiology, *Xenopus* oocytes were clamped at −60 mV using an OC-725 amplifier (Warner Instruments, Hamden, CT), Digidata 1322A, and the Strathclyde Electrophysiology Software Package (Department of Physiology and Pharmacology, University of Strathclyde, UK). Currents were recorded at a frequency of 5 kHz and filtered at 1 kHz. Microelectrode resistances ranged from 1.0 to 2.0 MΩ. Oocytes were perfused with saline at a constant rate of 12 ml/min. Drugs were applied via a simple gravity-fed system calibrated to run at the same rate. Extracellular saline contained 96 mM NaCl, 2 mM KCl, 1 mM $MgCl_2$, and 5 mM HEPES, pH 7.4, with NaOH). MTSEA was prepared immediately before each experiment and applied at a concentration of 2 mM for 2 min, followed by a 2-min wash, conditions that gave consistent and reproducible results.

Analysis and curve fitting was performed using Prism version 4.03 (GraphPad Software Inc., San Diego, CA). Concentration-response data for each oocyte were normalized to the maximum current for that oocyte. The mean and S.E.M. for a series of oocytes were plotted against agonist or antagonist concentration and iteratively fitted to eq. 1:

$$I_A = I_{min} + \frac{I_{max} - I_{min}}{1 + 10^{n_H(\log A_{50} - \log A)}} \quad (1)$$

where A is the concentration of ligand present, I_A is the current in the presence of ligand concentration A, I_{min} is the current when $A = 0$, I_{max} is the current when $A = \infty$, A_{50} is the concentration of A that evokes a current equal to $(I_{max} + I_{min})/2$, and n_H is the Hill coefficient. K_b was estimated from IC_{50} values using the Cheng-Prusoff equation with the modification by Leff and Dougall (1993) (eq. 2):

$$K_b = \frac{IC_{50}}{((2 + ([L]/[EC_{50}])^{n_H})^{1/n_H}) - 1} \quad (2)$$

where K_b is the dissociation constant of the competing drug, IC_{50} is the concentration of antagonist required to halve the maximal response, $[L]$ is the agonist concentration, $[EC_{50}]$ is the agonist concentration that elicits 50% of the maximal response, and n_H is the Hill slope of the agonist.

To perform cumulative inhibition experiments on 5-HT$_3$A receptors, two control (5-HT) measurements were made followed by a 1-min preapplication and then coapplication with 5-HT. The two control responses were used as the new maximal response from which the subsequent level of inhibition was calculated for each VUF10166 concentration.

Values are shown for a series of experiments and are presented as the mean ± S.E.M. Statistical analysis was performed in Prism using a Student's t test.

Radioligand Binding. Transfected HEK 293 cells were harvested into 1 ml of ice-cold HEPES buffer (10 mM, pH 7.4) and frozen. After thawing, they were washed with HEPES buffer and resuspended, and 50 μg of cell membranes was incubated in 0.5 ml of HEPES buffer containing [^{3}H]granisetron for 5-HT$_3$ receptor studies and [^{3}H]epibatidine for nACh receptor studies. Nonspecific binding

was determined using 10 μM *d*-tubocurarine or 3 mM nicotine, respectively. For competition binding (eight point), reactions were incubated for at least 30 h at 4°C. For 5-HT_3 receptor dissociation experiments, reactions were incubated with 1 nM [^{3}H]granisetron for 2 h before the addition of 100 μM VUF10166. Reactions were terminated by vacuum filtration using a Brandel cell harvester onto GF/B filters presoaked in 0.3% polyethyleneimine. Radioactivity was determined by scintillation counting using a Beckman BCLS6500 (Beckman Coulter, Fullerton, CA). Individual competition binding experiments were analyzed by iterative curve fitting using eq. 3 in Prism:

$$y = B_{min} + \frac{B_{max} - B_{min}}{1 + 10^{[L]-\log IC_{50}}} \quad (3)$$

where B_{min} is the nonspecific binding, B_{max} is the maximum binding, $[L]$ is the concentration of competing ligand, and IC_{50} is the concentration of competing ligand that blocks half of the specific bound radioligand. K_i values were estimated from IC_{50} values using the Cheng-Prusoff equation (eq. 4):

$$K_i = \frac{IC_{50}}{1 + [L]/K_d} \quad (4)$$

where K_i is the equilibrium dissociation constant for binding of the unlabeled antagonist, IC_{50} is the concentration of antagonist that blocks half the specific binding, $[L]$ is the free concentration of radioligand, and K_d is the equilibrium dissociation constant of the radioligand.

Values are shown for a series of experiments and are presented as the mean ± S.E.M. Statistical analysis was performed in Prism using a Student's *t* test.

Results

Radioligand Binding. The pK_d of [^{3}H]granisetron binding to 5-HT_3A (9.13 ± 0.04, K_d = 0.73 nM, n = 15) receptors was not significantly different from that for 5-HT_3AB receptors (9.09 ± 0.05, K_d = 0.81 nM, n = 4) ($p < 0.05$), consistent with previous reports (Brady et al., 2001). Competition binding of VUF10166 (Fig. 1B) with 1 nM [^{3}H]granisetron (~K_d) yielded pIC_{50} values of 9.98 ± 0.37 (IC_{50} = 0.10 nM, n = 25) at 5-HT_3A receptors and 7.30 ± 0.12 (IC_{50} = 50 nM, n = 9) at 5-HT_3AB receptors (Fig. 2A). This yielded significantly different ($p < 0.05$) pK_i values of 10.4 ± 0.37 (K_i = 0.04 nM) and 7.65 ± 0.12 (K_i = 22 nM) for 5-HT_3A and 5-HT_3AB receptors, respectively; Hill slopes for 5-HT_3A (0.97 ± 0.06) and 5-HT_3AB (1.08 ± 0.23) were similar ($p > 0.05$).

[^{3}H]Granisetron saturation binding curves were also examined in the presence of increasing concentrations of VUF10166. At 5-HT_3A receptors, the apparent K_d but not the B_{max} was increased by VUF10166, consistent with a competitive ligand (Fig. 2B). At 5-HT_3AB receptors, a rightward shift of the curve was also observed, but there was also a reduction in B_{max}, indicating a mechanism other than pure competition (Fig. 2C).

Dissociation of [^{3}H]granisetron in the presence of excess VUF10166 (100 μM) also revealed differences between homomeric and heteromeric receptors (Fig. 2D). At 5-HT_3A receptors, dissociation was best fit using a single exponential

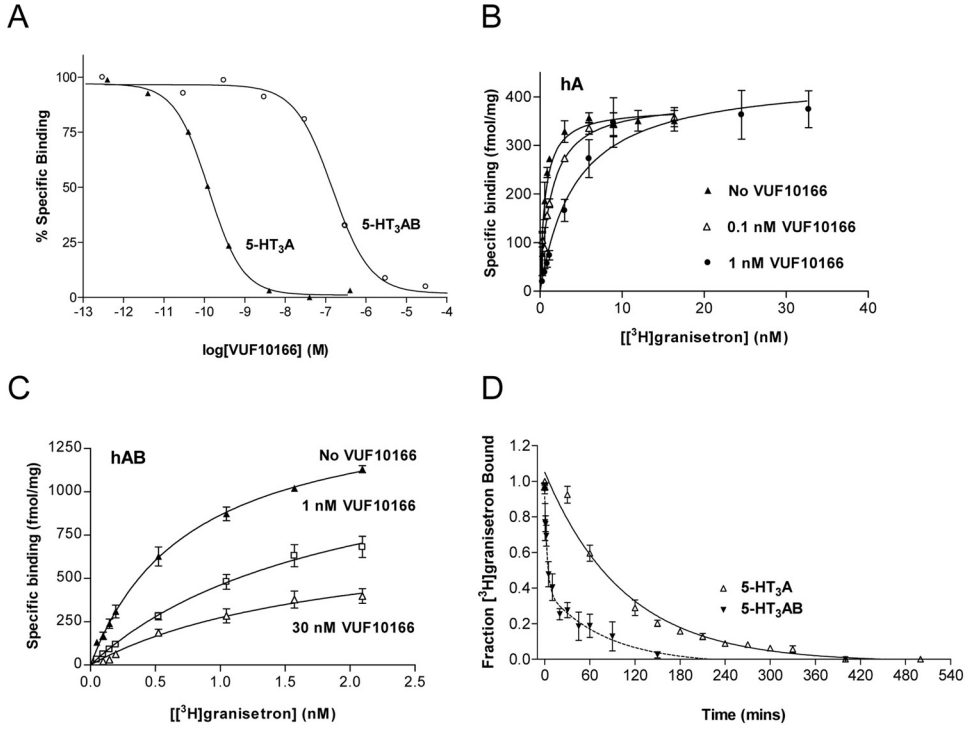

Fig. 2. Binding properties of VUF10166 at 5-HT_3A and 5-HT_3AB receptors expressed in HEK293 cells. A, typical experiments showing that the displacement of specific [^{3}H]granisetron binding by VUF10166 was different ($p > 0.05$) at 5-HT_3A and 5-HT_3AB receptors. B, [^{3}H]granisetron binding curves for wild-type 5-HT_3A receptors (K_d = 0.78 ± 0.16 nM, B_{max} = 382 ± 18 fmol/mg, n = 3) in the presence of 0.1 nM VUF10166 (K_d = 1.83 ± 0.30 nM*, B_{max} = 413 ± 21 fmol/mg, n = 3) and 1 nM VUF10166 (K_d = 4.32 ± 1.00 nM*, B_{max} = 443 ± 32 fmol/mg, n = 4). C, [^{3}H]granisetron binding curves for wild-type 5-HT_3AB receptors (K_d = 0.77 ± 0.05 nM, B_{max} = 1529 ± 40 fmol/mg, n = 4) and in the presence of 1 nM VUF10166 (K_d = 2.63 ± 0.96 nM, B_{max} = 1272 ± 392 fmol/mg, n = 3) and 30 nM (K_d = 1.89 ± 0.57 nM, B_{max} = 789 ± 135 fmol/mg*, n = 4). These concentrations are greater than or equal to the affinities of VUF10166 at 5-HT_3A (K_i = 0.04 nM) and 5-HT_3AB (K_i = 22.4 nM) receptors. D, dissociation of [^{3}H]granisetron after the addition of excess (100 μM) unlabeled VUF10166. Dissociation at the 5-HT_3A receptor was best fit with a single exponential ($t_{1/2}$ = 53.3 min), and 5-HT_3AB receptors were best fit with a double exponential ($t_{1/2}$ = 2.33 and 55.1 min). Sample sizes and rate constants can be found in the text. Values are mean ± S.E.M. *, significantly different from values for the wild type ($p < 0.05$).

($R^2 = 0.95$) with a rate constant of 0.013 ± 0.001 min^{-1} ($n = 7$, $t_{1/2} = 53.3$ min), and full dissociation was achieved in ~8 h. Dissociation from 5-HT$_3$AB receptors was best fit with a double exponential ($R^2 = 0.83$) with rate constants of 0.013 ± 0.009 min^{-1} ($n = 8$, $t_{1/2} = 55.1$ min) and 0.29 ± 0.11 min^{-1} ($t_{1/2} = 2.35$ min) and was complete within ~3 h. The slower dissociation rate in these 5-HT$_3$AB receptors is not significantly different from the value we observed in homomeric receptors ($p < 0.05$). These binding data show that VUF10166 competes with the specific 5-HT$_3$ receptor antagonist granisetron at both 5-HT$_3$A and 5-HT$_3$AB receptors, but that its mechanism at the latter cannot be described by competition alone.

Binding at nACh Receptors. There is some overlap between ligands that act at 5-HT$_3$ and nACh receptor binding sites (Gurley and Lanthorn, 1998; Macor et al., 2001; Drisdel et al., 2008). To determine whether VUF10166 has this characteristic, we examined its effects on [^{3}H]epabatidine binding to α7 nACh-5-HT$_3$ receptor chimeras expressed in HEK cells (Eiselé et al., 1993). At these receptors [^{3}H]epabatidine has a pK_d of 8.16 ± 0.06 ($n = 3$, $K_d = 6.9$ nM), but there was no displacement of 6 nM [^{3}H]epibatidine binding by VUF10166 at up to 100 μM ($n = 4$). These data indicate that VUF10166 has no action at the α7 nACh receptor binding site.

Antagonist Actions at 5-HT$_3$ Receptors. Oocytes expressing 5-HT$_3$A or 5-HT$_3$AB receptors respond to application of 5-HT with characteristics similar to those described previously (Table 1) (Thompson and Lummis, 2008). At 5-HT$_3$A receptors, inhibition of the 5-HT EC$_{50}$ response was seen at nanomolar concentrations of VUF10166, but inhibition was slow to develop and reverse, making it difficult to determine equilibrium measurements (e.g., IC$_{50}$). A cumulative inhibition protocol is illustrated in Fig. 3A, where a stable 2 μM 5-HT response (Fig. 3A, i) is reduced to ~50% following the preapplication of 30 nM VUF10166 for 1 min (Fig. 3A, ii). A subsequent application of 5-HT alone yields a response of similar amplitude (Fig. 3A, iii), which is itself reduced by ~50% upon a further application of 30 nM VUF10166 (Fig. 3A, iv). These and similar data suggest that the concentration of VUF10166 needed to inhibit 50% of the 5-HT-induced responses using this protocol is 37 nM, but this value is distinct from an IC$_{50}$. When VUF10166 is no longer applied, the recovery is slow, and 5-HT-induced responses are still significantly lower than the original 5-HT response after >10 min (Fig. 3A, v). Figure 3B shows the slow development of inhibition and slow recovery of the 5-HT$_3$A receptor with 3 nM VUF10166 and also demonstrates the effect of co- and preapplication on the inhibition; after a stable 5-HT response, a coapplication of 3 nM VUF10166 results in a smaller level of inhibition (Fig. 3B, a) than when VUF10166 is preapplied (Fig. 3B, b–e).

At 5-HT$_3$AB receptors, a 1 min co- or preapplication of VUF10166 resulted in stable levels of inhibition (Fig. 3, C and D). Recovery from inhibition of 5-HT$_3$AB receptors was achieved within 8 min, whereas at 5-HT$_3$A receptors, there was less than 60% recovery after 16 min (Fig. 3E). Thus, it is only possible to construct concentration-inhibition curves for 5-HT$_3$AB receptors (Fig. 3F), which yielded an IC$_{50}$ of 39.8 nM ($n = 7$, pIC$_{50} = 7.40 \pm 0.11$, $n_H = 0.65$), giving a K_b of 19 nM. These functional data support the radioligand binding data in showing distinct effects of VUF10166 at 5-HT$_3$A and 5-HT$_3$AB receptors.

The Pore Is Not Responsible for the Differing Actions of VUF10166. To date the only ligands that can distinguish 5-HT$_3$A from 5-HT$_3$AB receptors are those that bind in the receptor pore. To test whether VUF10166 binds at this location, we examined its effects in a receptor modified at the 6′ channel lining residue, which is critical for ligand binding in the pore (Das and Dillon, 2005; Thompson et al., 2011a). Receptors containing a T6′S substitution in the 5-HT$_3$A subunit had 5-HT concentration-response curves similar to those of wild-type receptors, as did heteromeric receptors with S6′T 5-HT$_3$B subunits (Fig. 4A). Recovery from VUF10166 inhibition (Fig. 4B) and inhibition curves (Fig. 4C) was also unaltered in the 6′ mutant receptors, suggesting that VUF10166 does not act in the pore. This hypothesis is supported by a lack of VUF10166 voltage dependence in both homomeric and heteromeric receptors, despite this ligand being charged at pH 7.4 (Fig. 4D).

Effects of 5-HT$_3$B Subunit Mutations on the Actions of VUF10166. To explore whether the actions of VUF10166 were mediated via residues in the 5-HT$_3$B subunit-containing binding pocket, we examined its properties at receptors containing 5-HT$_3$B subunit cysteine substitutions; these mutations were in either the principal (K181C, loop B) or the complementary (W90C, Q92C, loop D; Y153, loop E) faces (Fig. 1A). These mutations do not affect 5-HT-evoked currents or [^{3}H]granisetron binding (Thompson et al., 2011b).

Mutants were coexpressed in HEK293 cells with wild-type 5-HT$_3$A subunits, and dissociation of [^{3}H]granisetron was measured in the presence of excess VUF10166 (100 μM). Substitutions to the complementary face of the 5-HT$_3$B subunit resulted in dissociation rates for W90C ($n = 5$, 0.012 ± 0.001 min^{-1}, $t_{1/2} = 55.9$ min), Q92C ($n = 5$, 0.013 ± 0.002 min^{-1}, $t_{1/2} = 54.0$ min), and Y153C ($n = 3$, 0.014 ± 0.002

TABLE 1
Agonist properties derived from concentration-response curves
Data are means ± S.E.M.

Receptor	pEC$_{50}$	EC$_{50}$	Hill Slope	n	R_{max}
		μ*M*			
5-HT					
5-HT$_3$A	5.76 ± 0.03	1.73	2.56 ± 0.31	6	
5-HT$_3$AB	4.56 ± 0.03*	27.6	1.05 ± 0.09*	12	
VUF10166					
5-HT$_3$A	5.28 ± 0.14	5.20	1.24 ± 0.37	9	0.24 ± 0.02†
5-HT$_3$AB	NR	NR	NR	3	

R_{max}, maximal current amplitude for the test ligand compared with the maximal current amplitude for 5-HT.
* Significantly different from wild-type 5-HT$_3$A receptors, $p < 0.05$.
† Significantly different from the maximal 5-HT current, $p < 0.05$.
NR, no reported value because 5-HT$_3$AB receptor responses were too small to determine if there was a significant response.

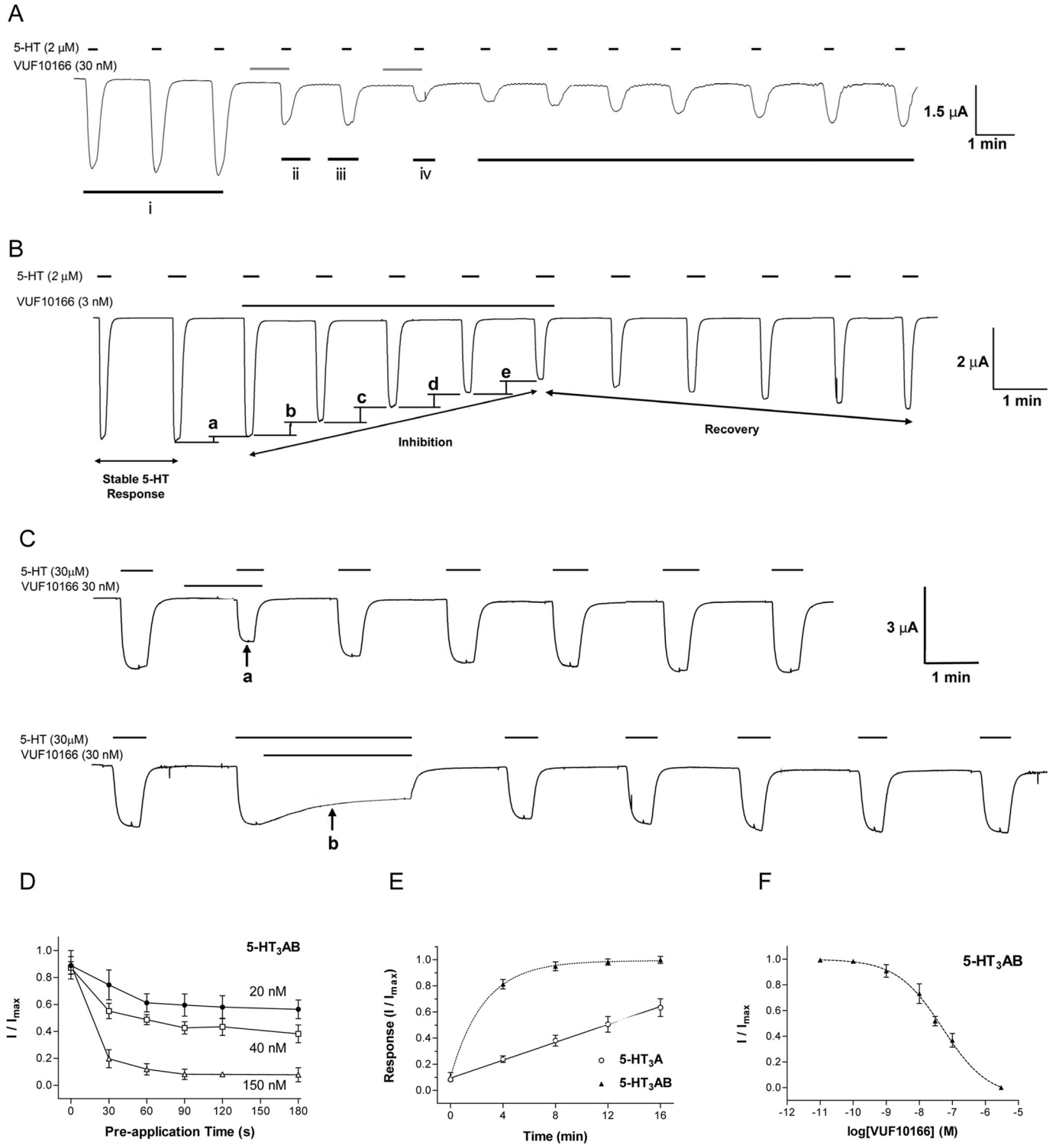

Fig. 3. Inhibition of 5-HT_3 receptor responses by VUF10166. A, typical 5-HT_3A receptor responses. 5-HT (2 μM) was applied three times at 1-min intervals to show that the response is stable (i), 30 nM VUF10166 reduces the maximal current to ~50% of its initial value (ii), and the response has a similar amplitude with the next application of 5-HT alone (iii). A further application of 30 nM VUF10166 reduces the current by ~50% again (iv), and the subsequent 5-HT responses show slow recovery. B, a typical trace showing inhibition and recovery of a 5-HT_3A receptor response with 3 nM VUF10166. First, a stable 2 μM 5-HT response is recorded. Coapplication of 5-HT and VUF10166 reduces the maximal current. Increasing inhibition is observed during subsequent 5-HT applications, and the response slowly recovers when the VUF10166 is removed. These data also show that coapplication reduces the response by 7% (a), which is less than the 14% reduction that is seen when the same concentration of VUF10166 is preapplied (b, c, d, and e). C, at 5-HT_3AB receptors, maximal VUF10166 inhibition reaches a stable level after a 1-min application whether VUF10166 (30 nM) is preapplied (a) or coapplied (b), and recovery is similar. D, at 5-HT_3AB receptors, maximal VUF10166 inhibition is reached after a 1-min application. E, recovery from VUF10166 application was slower at 5-HT_3A than at 5-HT_3AB receptors; 5-HT_3AB receptors recovered from inhibition within 8 min, whereas recovery for 5-HT_3A receptor responses is >25 min. F, a VUF10166 concentration-inhibition curve at 5-HT_3AB receptors. Values are mean ± S.E.M., with sample size and other parameters shown in the text and tables.

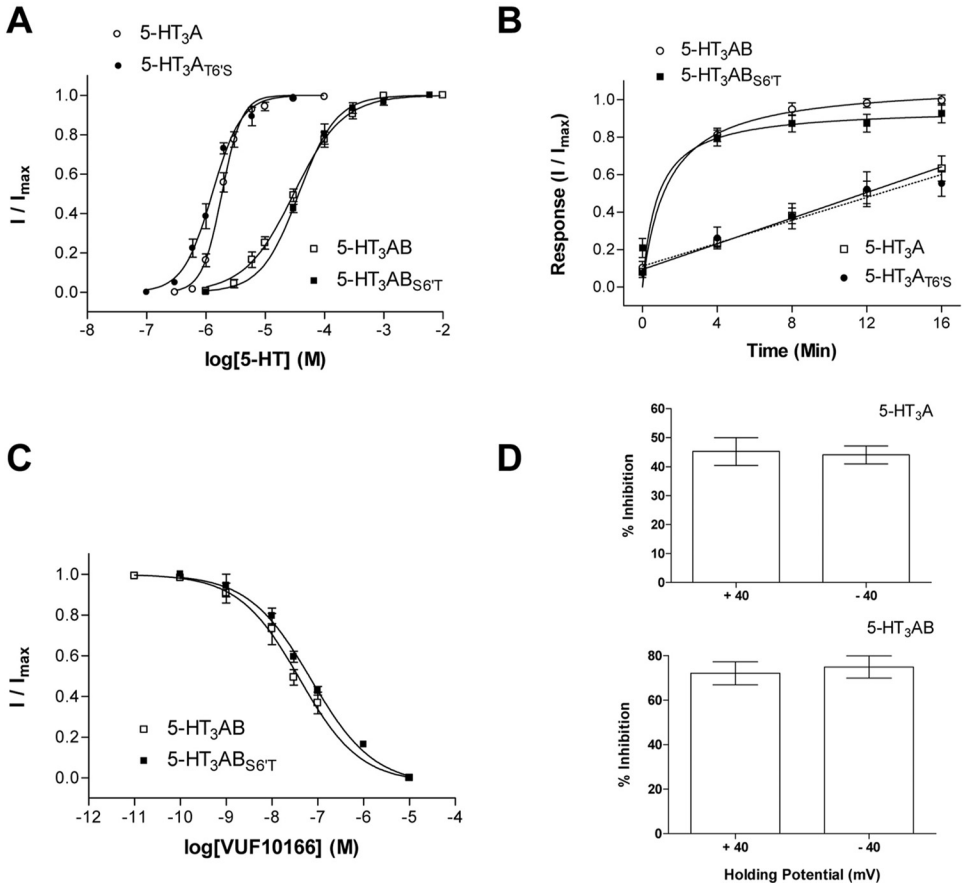

Fig. 4. The effects of 6′ channel substitutions on VUF10166 properties. A, wild-type receptors (table 1) had 5-HT sensitivity similar to that of their 5-HT$_3$A$_{T6'S}$ (pEC_{50} = 5.88 ± 0.03, EC_{50} = 1.3 μM, n_H = 1.8, n = 4) and 5-HT$_3$AB$_{S6'T}$ (pEC_{50} = 4.43 ± 0.04, EC_{50} = 37 μM, n_H = 1.4, n = 8) counterparts ($p > 0.05$). B, recovery from VUF10166 inhibition was unaltered by $A_{T6'S}$ or $B_{S6'T}$ substitutions. C, VUF10166 inhibition of heteromeric receptors was the same ($p > 0.05$) for wild-type (table 3) and 5-HT$_3$AB$_{S6'T}$ mutants (pIC_{50} = 7.15 ± 0.10, IC_{50} = 71 nM, n_H = 0.63, n = 7). D, voltage-dependence of VUF10166 inhibition at +40mV and −40 mV was the same for both 5-HT$_3$A and 5-HT$_3$AB wild-type receptors ($p > 0.05$), consistent with a compound that does not block the channel. All values presented in Fig. 4 are the mean ± S.E.M.

min^{-1}, $t_{1/2}$ = 48.8 min) that were not significantly different ($p < 0.05$) from those measured at wild-type 5-HT$_3$A receptors (Fig. 5). K181C substitution yielded data that were best fit by a double exponential with slow (0.008 ± 0.011 min^{-1}, $t_{1/2}$ = 85.3 min) and fast (0.047 ± 0.013 min^{-1}, $t_{1/2}$ = 14.8 min, n = 4) components that were not significantly different from those measured at wild-type 5-HT$_3$AB receptors ($p < 0.05$).

The pattern of change was identical using MTSEA modification of cysteine mutants expressed in oocytes (Fig. 6). There were no changes in 5-HT parameters after MTSEA treatment of modified residues (Table 2), but MTSEA application to receptors containing complementary face substitutions resulted in a reduction in the extent of recovery of VUF10166 inhibition (Fig. 6, A and B; Table 3). Substitutions on the principal face caused no change to the VUF10166 concentration-inhibition curve or the recovery from inhibition after MTSEA treatment (Fig. 6, E–H; Table 3). These data are consistent with our radioligand measurements, showing that only substitutions to the complementary face of the 5-HT$_3$B subunit alter the properties of VUF10166. In these mutant receptors, the properties of VUF10166 were similar to those measured at wild-type homomers.

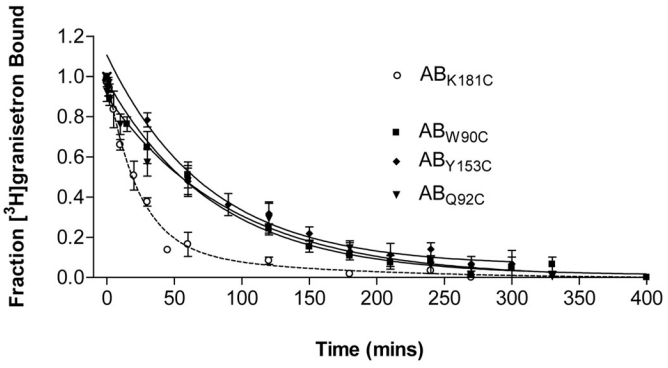

Fig. 5. Complementary face mutations alter the rate of [^{3}H]granisetron dissociation in the presence of VUF10166. W90C, Q92C, and Y153C substitutions in the complementary face of the 5-HT$_3$B subunit produce mutant heteromeric receptors with rates of dissociation that resemble those found in homomeric receptors (Fig. 2D). In contrast, K181C in the principal face produced receptors with dissociation rates similar to those of the wild-type heteromer. Values are the mean ± S.E.M. Sample size and rate constants for these curves can be found in the text.

VUF10166 Acts as a Partial Agonist at 5-HT$_3$A Receptors. In addition to its antagonist properties, VUF10166 at higher concentrations acts as a partial agonist at 5-HT$_3$A receptors, with an EC_{50} of 5.2 μM and R_{max} of 0.24 (Fig. 7; Table 1). This high concentration agonist response preceded the usual antagonist effect, and sustained exposure at these higher concentrations inhibited subsequent 5-HT responses. Small ($R_{max} < 0.03$) responses to 100 μM VUF10166 were seen at 5-HT$_3$AB receptors, but because this compound has limited solubility, we were unable to test higher concentrations (Fig. 7). Therefore, our data do not preclude VUF10166 partial agonist activity at 5-HT$_3$AB receptors but, if it exists, such activity would have an EC_{50} considerably higher than that at 5-HT$_3$A receptors.

Discussion

VUF10166 is a high-affinity 5-HT$_3$ receptor antagonist that was originally identified from a fragment library screen

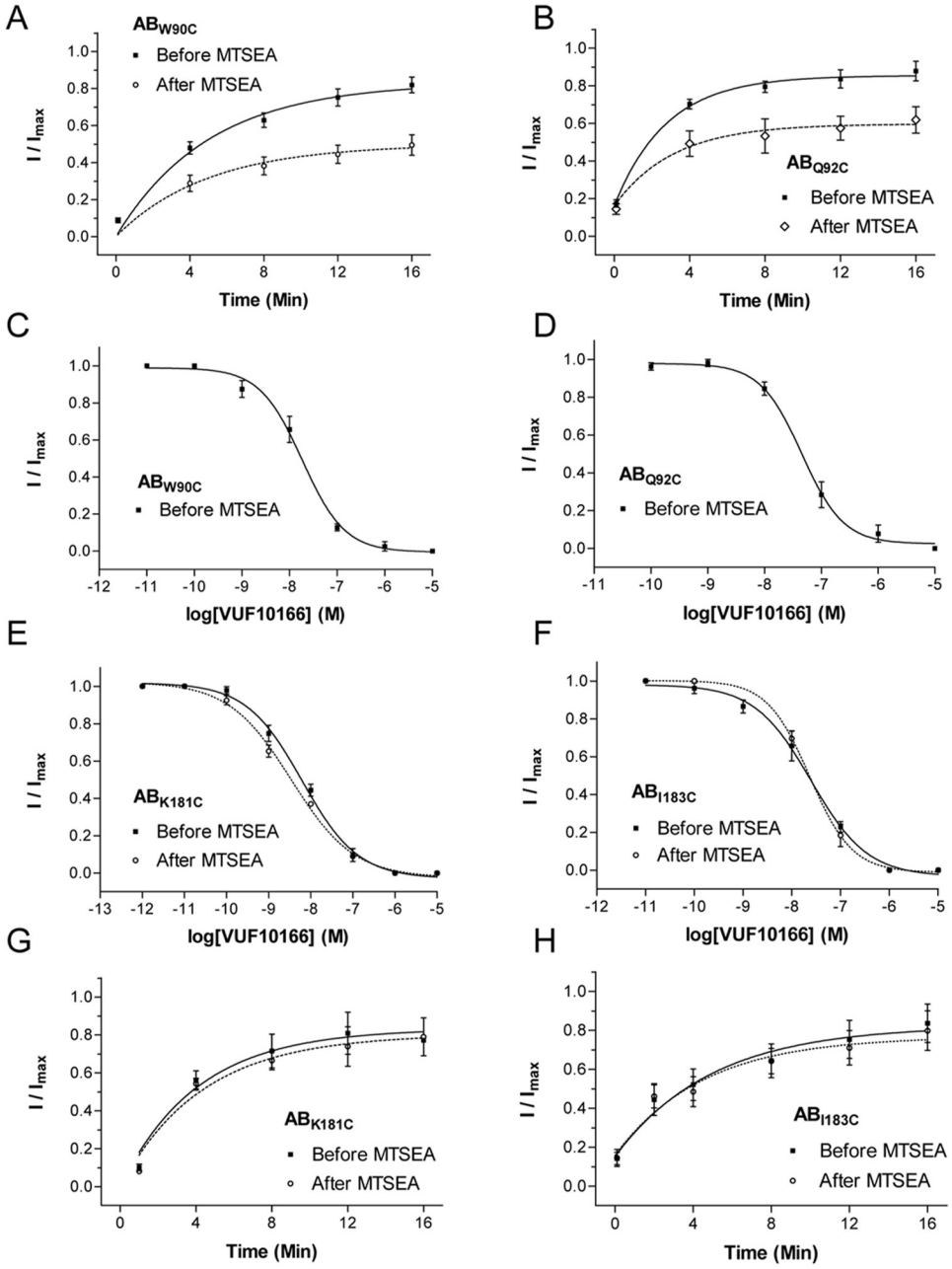

Fig. 6. The effects of 5-HT$_3$B subunit mutations on VUF10166 inhibition. Mutations to the complementary (−) face of the B subunit caused a change in the extent of recovery from inhibition after MTSEA modification (A and B). Because MTSEA treatment of these mutants produced receptors that were more A-like, it was not possible to measure IC_{50} values after modification (C and D). MTSEA treatment of receptors containing cysteine mutations in the principal (+) face of the B subunit had no effect on the VUF10166 IC_{50} (E and F) or extent of recovery (G and H) from VUF10166 inhibition. Values are the mean ± S.E.M. Rate constants and sample size are shown in Table 3.

(Thompson et al., 2010b). Here, radioligand binding studies show that this compound acts as a competitive antagonist at 5-HT$_3$A receptors with subnanomolar affinity (K_i = 0.04 nM), indicating activity comparable to that of some of the most potent 5-HT$_3$ receptor antagonists characterized to date (Thompson and Lummis, 2007; Walstab et al., 2010). The affinity at 5-HT$_3$AB receptors was significantly lower (K_i = 22 nM) and did not show purely competitive behavior. This is unusual because known competitive 5-HT$_3$A receptor antagonists have similar affinities at homomeric and heteromeric receptors. The roles of 5-HT$_3$A and 5-HT$_3$AB receptors are not yet clear but given the clinical importance of Cys-loop receptor subtypes (e.g., the high-affinity benzodiazepine binding site is only found on GABA$_A$ receptors containing a γ2 subunit), this information could assist not only in our understanding of the roles of these receptors but also in the design of more selective and effective therapeutic agents.

To probe the VUF10166 binding site, we examined its effects in radioligand binding studies. Increasing concentrations of VUF10166 at 5-HT$_3$A receptors were accompanied by a surmountable rightward shift of the [^{3}H]granisetron saturation binding curve, indicating competition. At 5-HT$_3$AB receptors, VUF10166 caused a similar rightward shift but also a reduction in B_{max}, suggesting that incorporation of the 5-HT$_3$B subunit creates an additional site of action. Further evidence for this comes from dissociation studies, which indicate two binding sites for VUF10166 at 5-HT$_3$AB receptors. VUF10166 can therefore be added to the list of ligands that can distinguish between 5-HT$_3$A and 5-HT$_3$AB receptors. Existing compounds include picrotoxin, ginkgolide A, ginkgolide B, chloroquine, and mefloquine, but all of these compounds act in the pore, with their different potencies resulting from the differing M2 residues in homomeric and heteromeric receptor pores (Das and Dillon, 2005; Thompson

TABLE 2
5-HT agonist parameters before and after MTSEA treatment
Data are means ± S.E.M. No data were significantly different before and after MTSEA ($p > 0.05$).

Mutant	pEC_{50}	EC_{50}	n_H	n
		μM		
Before MTSEA				
Wild type				
AB	4.56 ± 0.03	27.6	1.05 ± 0.09	12
B loop				
AB_{K181C}	4.43 ± 0.09	36.8	0.82 ± 0.11	8
AB_{I183C}	4.63 ± 0.09	23.4	0.83 ± 0.16	3
D loop				
AB_{Q92C}	4.77 ± 0.08	16.9	1.03 ± 0.20	4
AB_{W90C}	5.07 ± 0.07	8.43	1.06 ± 0.16	5
After MTSEA				
Wild type				
AB	4.68 ± 0.04	20.9	1.06 ± 0.13	4
B loop				
AB_{K181C}	4.51 ± 0.12	30.7	0.76 ± 0.19	4
AB_{I183C}	4.79 ± 0.07	16.3	1.26 ± 0.24	3
D loop				
AB_{Q92C}	4.69 ± 0.12	20.3	0.70 ± 0.15	3
AB_{W90C}	5.13 ± 0.08	7.42	1.16 ± 0.29	3

TABLE 3
VUF10166 antagonist parameters before and after MTSEA treatment
Data are means ± S.E.M. No significant differences were found ($p > 0.05$) for pIC_{50} values before and after MTSEA where measured.

Mutant	pIC_{50}	IC_{50}	n_H	n	Recovery Rate	n
		nM			min^{-1}	
Before MTSEA						
Wild-type						
AB	7.43 ± 0.03	37.5	1.60	7	0.39 ± 0.02	5
B loop						
AB_{K181C}	8.21 ± 0.08	6.23	0.70	4	0.24 ± 0.06	3
AB_{I183C}	7.61 ± 0.09	24.7	0.75	3	0.21 ± 0.09	6
D loop						
AB_{Q92C}	7.34 ± 0.07	45.3	1.19	4	0.36 ± 0.06	4
AB_{W90C}	7.73 ± 0.07	18.4	0.97	9	0.22 ± 0.03	14
After MTSEA						
Wild-type						
AB	7.44 ± 0.05	36.0	1.2	3	0.27 ± 0.08	3
B loop						
AB_{K181C}	8.50 ± 0.05	3.47	0.58	3	0.23 ± 0.06	3
AB_{I183C}	7.58 ± 0.06	26.5	1.09	3	0.22 ± 0.09	3
D loop						
AB_{Q92C}	NR					
AB_{W90C}	NR					

NR, no reported value because the recovery from inhibition was too slow to determine an IC_{50}.

et al., 2011a). VUF10166 is unlikely to bind in the pore because the partial agonist response at high concentrations shows that the channel is not blocked, and its effects are not voltage-dependent. To confirm this, we exchanged the 6′ channel lining residues in 5-HT$_3$A and 5-HT$_3$B subunits, because this residue interacts with all of the channel-binding compounds described to date (Das and Dillon, 2005; Thompson et al., 2011a). The properties of VUF10166 were not altered by these mutations, providing further evidence that it does not act within the pore.

To determine whether VUF10166 acts in a 5-HT$_3$B subunit-containing binding pocket, we made cysteine substitutions in either the principal (+) or complementary (−) face of this subunit. Mutations W90C, Q92C, and Y153C in the B interface produced 5-HT$_3$AB receptors with radioligand binding properties resembling those of wild-type homomeric receptors. Electrophysiological studies supported this finding because only W90C and Q92C mutants showed altered recovery from VUF10166 inhibition after MTSEA modification. In contrast, radioligand dissociation and recovery from inhibition were unaltered by B+ substitutions. These data indicate a role of the A+B− interface in VUF10166 actions. This interface was originally considered the major agonist binding site in 5-HT$_3$AB receptors (Barrera et al., 2005), but more recent work has shown that an A+A− interface is required for function in both homomeric and heteromeric receptors (Lochner and Lummis, 2010; Thompson et al., 2011b). We propose that VUF10166 binds to this A+A− interface in both 5-HT$_3$A and 5-HT$_3$AB receptors, with an A+B− interface acting as a modulatory site; we suggest that binding to this A+B− site allosterically influences ligands bound to the A+A− site, resulting in faster dissociation and recovery. This is illustrated in Fig. 8, which shows that VUF10166 and other competitive ligands bind to a common A+A− interface in both receptor types, explaining why both receptors have identical [^{3}H]granisetron affinities and why they share a common rate of [^{3}H]granisetron dissociation in the presence of unlabeled VUF10166.

At high concentrations VUF10166 also acts as a partial agonist at 5-HT$_3$A receptors, but we could not identify a similar

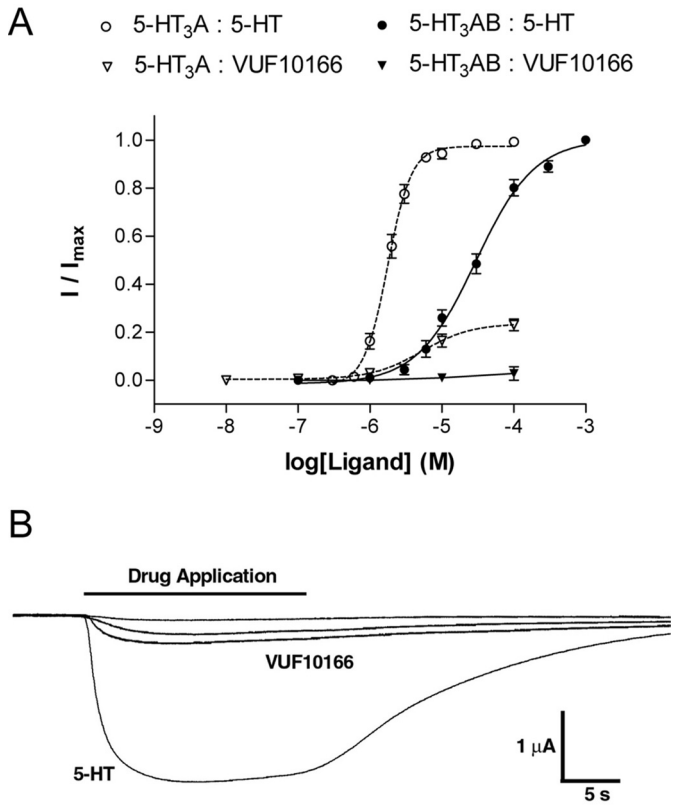

Fig. 7. Agonist actions of 5-HT and VUF10166 at 5-HT_3A and 5-HT_3AB receptors. A, concentration-response curves showing the agonist response to 5-HT and VUF10166 at 5-HT_3A receptors. VUF10166 activation of 5-HT_3AB receptors was negligible (R_{max} = 0.03 ± 0.02, n = 3). B, examples of traces at 1, 10, and 100 μM VUF10166 are compared with a maximal (30 μM) 5-HT response at 5-HT_3A receptors. Parameters derived from these curves are shown in Table 1.

action at 5-HT_3AB receptors. VUF10166 shares these unusual partial agonist/antagonist properties with *N*-[(3*S*)-1-azabicyclo[2.2.2]oct-3-yl]-1*H*-indazole-3-carboxamide hydrochloride (RG3487), an α7 nACh receptor ligand that is currently undergoing phase II clinical trials for the treatment of Alzheimer's disease (Wallace et al., 2011). Like VUF10166, RG3487 is a high-affinity antagonist after sustained exposure, with partial agonist activity at higher concentrations. RG3487 also has a nanomolar affinity for inhibiting 5-HT-induced responses and displacing [^{3}H]granisetron binding, although activation of 5-HT_3 receptors was not reported. VUF10166 does not have similar activity at α7 nACh receptors because a 100 μM concentration did not inhibit [^{3}H]epibatidine binding.

A dual action agonist-antagonist effect is thought to underpin the therapeutic efficiency of the nACh receptor partial agonist varenicline. However, this antagonism relies on the ability of the partial agonist to compete with the native ligand, which enforces a reduced, but controlled, activation of the nACh receptor. Therefore, the "antagonism" is solely the suppression of the full agonist response when both partial and full agonists are present (Rollema et al., 2007). In contrast, VUF10166 antagonism was seen at far lower concentrations (>1000-fold) than those needed for the partial agonist response. Similar inhibitory effects have been seen for low concentrations of nicotinic agonists owing to the slow accumulation of desensitized receptors, and it is possible that this mechanism also underlies the actions of VUF10166 at low concentrations (Fenster et al., 1999; Paradiso and Steinbach, 2003; Deiml et al., 2004; Yu et al., 2009).

In summary, we have shown that VUF10166 is a novel and highly potent 5-HT_3A receptor antagonist. At 5-HT_3AB receptors, it is also an antagonist but is less potent. [^{3}H]Granisetron binding shows that VUF10166 binds to the orthosteric (A+A−) binding site in these receptors, but changes resulting from B− substitutions suggest a second binding site in the heteromeric receptor. This subtype specificity extends the range of compounds that can distinguish between homomeric and heteromeric 5-HT_3 receptors, but, uniquely, this difference is not a consequence of binding within the channel. At higher concentrations VUF10166 also acts as a partial agonist. Such unusual properties could have potential therapeutic uses. 5-HT_3 receptor antagonists have a range of clinical applications and partial agonists are also being considered (Kawano et al., 2005; Yoshida et al., 2005; Thompson et al., 2007; Walstab et al., 2010). The combination of 5-HT_3 receptor subtype selectivity, high potency, and allosterism shown here suggest that this compound has considerable potential.

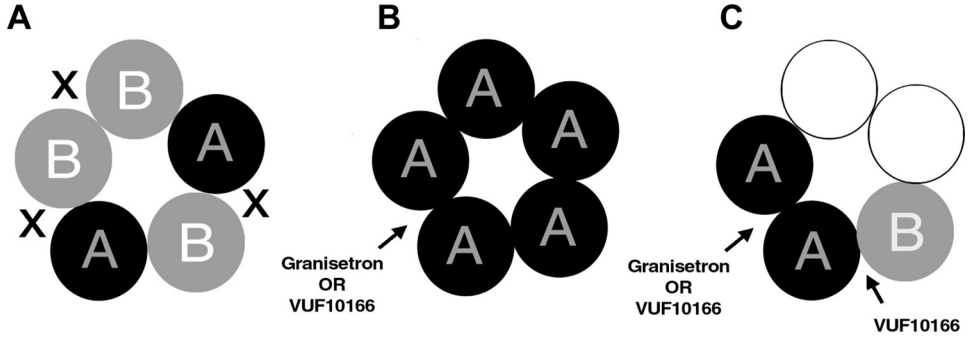

Fig. 8. A cartoon showing potential binding sites for VUF10166 and granisetron in 5-HT_3 receptors with different stoichiometries. A, 5-HT_3AB receptor stoichiometry as proposed by Barrera et al. (2005). In this model [^{3}H]granisetron and other competitive ligands bind at the A+B− interface in a similar way to that at the A+A− interface in the homomeric receptor (Moura Barbosa et al., 2010). X shows the sites containing B+ interfaces that are not affected by substitutions. Because this leaves only the A+B− sites, this model cannot explain the different affinities of VUF10166 at 5-HT_3A and 5-HT_3AB receptors described in this study. B, the homomeric 5-HT_3A receptor has five identical A+A− binding sites to which [^{3}H]granisetron and VUF10166 can bind competitively, as shown in this study. C, a 5-HT_3AB receptor with an A+A− binding site (Lochner and Lummis, 2010; Thompson et al., 2011b). In this model VUF10166 binds to both A+A− and A+B− interfaces where it acts competitively (A+A−) or allosterically (A+B−). The data in this study support this model. Two subunits have been omitted because they cannot be defined from the data presented here.

Acknowledgments

We thank Linda Silvestri for excellent technical assistance.

Authorship Contributions

Participated in research design: Thompson and Lummis.

Conducted experiments: Thompson.

Contributed new reagents or analytic tools: Verheij and de Esch.

Performed data analysis: Thompson.

Wrote or contributed to the writing of the manuscript: Thompson, Lummis, Verheij, and de Esch.

Other: Lummis and de Esch.

References

Barnes NM, Hales TG, Lummis SC, and Peters JA (2009) The 5-HT$_3$ receptor—the relationship between structure and function. *Neuropharmacology* **56:**273–284.

Barrera NP, Herbert P, Henderson RM, Martin IL, and Edwardson JM (2005) Atomic force microscopy reveals the stoichiometry and subunit arrangement of 5-HT$_3$ receptors. *Proc Natl Acad Sci USA* **102:**12595–12600.

Brady CA, Stanford IM, Ali I, Lin L, Williams JM, Dubin AE, Hope AG, and Barnes NM (2001) Pharmacological comparison of human homomeric 5-HT$_3$A receptors versus heteromeric 5-HT$_3$A/$_3$B receptors. *Neuropharmacology* **41:**282–284.

Das P and Dillon GH (2005) Molecular determinants of picrotoxin inhibition of 5-hydroxytryptamine type 3 receptors. *J Pharmacol Exp Ther* **314:**320–328.

Davies PA, Pistis M, Hanna MC, Peters JA, Lambert JJ, Hales TG, and Kirkness EF (1999) The 5-HT$_3$B subunit is a major determinant of serotonin-receptor function. *Nature* **397:**359–363.

Deiml T, Haseneder R, Zieglgänsberger W, Rammes G, Eisensamer B, Rupprecht R, and Hapfelmeier G (2004) α-Thujone reduces 5-HT$_3$ receptor activity by an effect on the agonist-reduced desensitization. *Neuropharmacology* **46:**192–201.

Drisdel RC, Sharp D, Henderson T, Hales TG, and Green WN (2008) High affinity binding of epibatidine to serotonin type 3 receptors. *J Biol Chem* **283:**9659–9665.

Eiselé JL, Bertrand S, Galzi JL, Devillers-Thiéry A, Changeux JP, and Bertrand D (1993) Chimaeric nicotinic-serotonergic receptor combines distinct ligand binding and channel specificities. *Nature* **366:**479–483.

Fenster CP, Hicks JH, Beckman ML, Covernton PJ, Quick MW, and Lester RA (1999) Desensitization of nicotinic receptors in the central nervous system. *Ann NY Acad Sci* **868:**620–623.

Goldin LR (1992) Maintenance of *Xenopus laevis* and oocyte injection, in *Methods in Enzymology* (Rudy B and Iverson LE eds), vol 207, pp 267–279, Academic Press, New York.

Gurley DA and Lanthorn TH (1998) Nicotinic agonists competitively antagonize serotonin at mouse 5-HT$_3$ receptors expressed in *Xenopus* oocytes. *Neurosci Lett* **247:**107–110.

Holbrook JD, Gill CH, Zebda N, Spencer JP, Leyland R, Rance KH, Trinh H, Balmer G, Kelly FM, Yusaf SP, et al. (2009) Characterisation of 5-HT3C, 5-HT3D and 5-HT3E receptor subunits: evolution, distribution and function. *J Neurochem* **108:**384–396.

Jensen AA, Davies PA, Bräuner-Osborne H, and Krzywkowski K (2008) 3B but which 3B and that's just one of the questions: the heterogeneity of human 5-HT$_3$ receptors. *Trends Pharmacol Sci* **29:**437–444.

Kawano K, Mori T, Fu L, Ito T, Niisato T, Yoshida S, Shiokawa S, Sato Y, Murakami H, and Shishikura T (2005) Comparison between partial agonist (ME3412) and antagonist (alosetron) of 5-hydroxytryptamine 3 receptor on gastrointestinal function. *Neurogastroenterol Motil* **17:**290–301.

Leff P and Dougall IG (1993) Further concerns over Cheng-Prusoff analysis. *Trends Pharmacol Sci* **14:**110–112.

Liman ER, Tytgat J, and Hess P (1992) Subunit stoichiometry of a mammalian K^+ channel determined by construction of multimeric cDNAs. *Neuron* **9:**861–871.

Lochner M and Lummis SC (2010) Agonists and antagonists bind to an A-A interface in the heteromeric 5-HT$_3$AB receptor. *Biophys J* **98:**1494–1502.

Macor JE, Gurley D, Lanthorn T, Loch J, Mack RA, Mullen G, Tran O, Wright N, and Gordon JC (2001) The 5-HT$_3$ antagonist tropisetron (ICS 205-930) is a potent and selective α7 nicotinic receptor partial agonist. *Bioorg Med Chem Lett* **11:**319–321.

Moura Barbosa AJ, De Rienzo F, Ramos MJ, and Menziani MC (2010) Computational analysis of ligand recognition sites of homo- and heteropentameric 5-HT$_3$ receptors. *Eur J Med Chem* **45:**4746–4760.

Niesler B, Walstab J, Combrink S, Möller D, Kapeller J, Rietdorf J, Bönisch H, Göthert M, Rappold G, and Brüss M (2007) Characterization of the novel human serotonin receptor subunits 5-HT$_3$C, 5-HT$_3$D, and 5-HT$_3$E. *Mol Pharmacol* **72:**8–17.

Paradiso KG and Steinbach JH (2003) Nicotine is highly effective at producing desensitization of rat α4β2 neuronal nicotinic receptors. *J Physiol* **553:**857–871.

Rollema H, Chambers LK, Coe JW, Glowa J, Hurst RS, Lebel LA, Lu Y, Mansbach RS, Mather RJ, Rovetti CC, et al. (2007) Pharmacological profile of the α4β2 nicotinic acetylcholine receptor partial agonist varenicline, an effective smoking cessation aid. *Neuropharmacology* **52:**985–994.

Thompson AJ, Duke RK, and Lummis SC (2011a) Binding sites for bilobalide, diltiazem, ginkgolide, and picrotoxinin at the 5-HT$_3$ receptor. *Mol Pharmacol* **80:**183–190.

Thompson AJ, Lester HA, and Lummis SC (2010a) The structural basis of function in Cys-loop receptors. *Q Rev Biophys* **43:**449–499.

Thompson AJ, Lochner M, and Lummis SC (2007) The antimalarial drugs quinine, chloroquine and mefloquine are antagonists at 5-HT$_3$ receptors. *Br J Pharmacol* **151:**666–677.

Thompson AJ and Lummis SC (2007) The 5-HT$_3$ receptor as a therapeutic target. *Expert Opin Ther Targets* **11:**527–540.

Thompson AJ and Lummis SC (2008) Antimalarial drugs inhibit human 5-HT$_3$ and GABA$_A$ but not GABA$_C$ receptors. *Br J Pharmacol* **153:**1686–1696.

Thompson AJ, Price KL, and Lummis SC (2011b) Cysteine modification reveals which subunits form the ligand binding site in human heteromeric 5-HT$_3$AB receptors. *J. Physiol* **589:**4243–4257.

Thompson AJ, Verheij MH, Leurs R, De Esch IJ, and Lummis SC (2010b) An efficient and information-rich biochemical method design for fragment library screening on ion channels. *Biotechniques* **49:**822–829.

Wallace TL, Callahan PM, Tehim A, Bertrand D, Tombaugh G, Wang S, Xie W, Rowe WB, Ong V, Graham E, et al. (2011) RG3487, a novel nicotinic α7 receptor partial agonist, improves cognition and sensorimotor gating in rodents. *J Pharmacol Exp Ther* **336:**242–253.

Walstab J, Rappold G, and Niesler B (2010) 5-HT$_3$ receptors: role in disease and target of drugs. *Pharmacol Ther* **128:**146–169.

Yoshida S, Shiokawa S, Kawano K, Ito T, Murakami H, Suzuki H, and Sato Y (2005) Orally active benzoxazole derivative as 5-HT$_3$ receptor partial agonist for treatment of diarrhea-predominant irritable bowel syndrome. *J Med Chem* **48:**7075–7079.

Yu KD, Liu Q, Wu J, and Lukas RJ (2009) Kinetics of desensitization and recovery from desensitization for human α4β2-nicotinic acetylcholine receptors stably expressed in SH-EP1 cells. *Acta Pharmacol Sin* **30:**805–817.

Address correspondence to: Dr. Sarah C. R. Lummis, Department of Biochemistry, Tennis Court Road, Cambridge CB2 1QW, UK. E-mail: sl120@cam.ac.uk